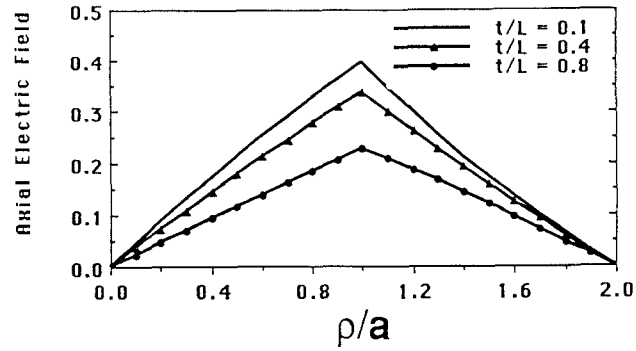

Fig. 4. Variation of the axial electric field with ρ/a and t/L; $b/a = 2.0$, $\epsilon_{r2} = 2.56$.

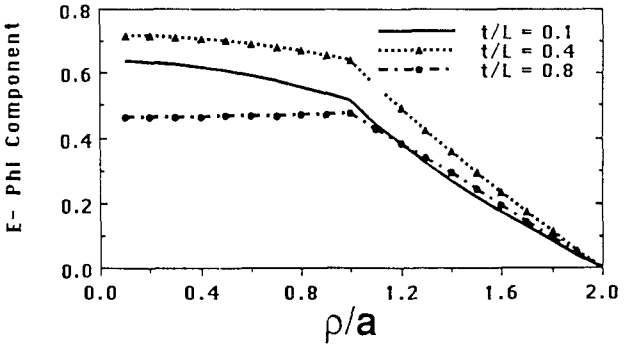

Fig. 5. Variation of the circumferential electric field with ρ/a and t/L; $b/a = 2.0$, $\epsilon_{r2} = 2.56$.

same t/L ratio and k_0a, the normalized phase constant increases with increasing corrugation depth. Fig. 3 shows the variation of β/k_0 with t/L for a larger value of k_0a. Increasing k_0a appears to result in a larger value of β/k_0 for the same t/L ratio. When all the physical parameters and the permittivity remain unchanged, increasing k_0a corresponds to an increase in frequency. Hence, an increase in frequency acts to slow down the propagating wave in a cylindrical waveguide loaded with dielectric disks. Consequently, the ratio β/k_0 approaches unity for a smaller value if k_0a is larger. We can also view the disk-loaded cylindrical waveguide as a band-pass filter and these results indicate that an increase in frequency would lead to a narrowing of the bandwidth.

Fig. 4 shows the variation of the axial component E_z with the normalized radius for three different values of the thickness ratio. The axial electric field is zero on the axis, increases slowly in region 1 to a maximum value, decreases in region 2, and finally vanishes at the conducting boundary at $\rho = b$. The magnitude of the electric field decreases with increasing t/L ratio.

Fig. 5 shows the variation of the circumferential electric field component in the transverse plane. The ϕ component starts at a constant value on the axis and is almost constant in region 1 for larger t/L ratios. For lower values of t/L, however, it tends to decrease slightly. In region 2, it decreases monotonically and at the conducting boundary it goes to zero. Once again, we notice that the magnitude is higher for higher values of the thickness ratio. The variations of the axial and circumferential components of the electric field with respect to the angular coordinate ϕ are given by $\cos\phi$ and $\sin\phi$, respectively.

IV. Conclusions

The problem of guided wave propagation in a circular waveguide with a corrugated dielectric lining is solved by a boundary value problem by regarding the medium between the corrugations as a medium with tensor permittivity. By matching the field components at the boundaries, the characteristic equation for the phase constant is derived. This characteristic equation, which is transcendental in nature, is numerically solved for a given set of physical parameters, for example the diameter of the cylinder, the corrugation depth, the thickness ratio, and the permittivity of the dielectric material. Some representative results of the normalized phase constant and its variation with different parameters are shown. The variations of the axial and circumferential electric field components in the transverse plane with the normalized radius are shown for different values of the thickness ratio.

References

[1] A. F. Kay, "The scalar feed," US Air Force Cambridge Research Laboratories Report, AD60169, pp. 62–347, Mar. 1964.
[2] H. C. Minnett and B. M. Thomas, "Fields in the image space of symmetrical focussing reflectors," *Proc. Inst. Elec. Eng.*, vol. 115, no. 10, pp. 1419–1430. Oct. 1968.
[3] P. J. B. Clarricoats and P. K. Saha, "Propagation and radiation behavior of corrugated feeds, Part. 1: Corrugated waveguide feeds," *Proc. Inst. Elec Eng.*, vol. 118, no. 9, pp. 1167–1176, Sept. 1971.
[4] A. Kumar, "Dielectric lined circular waveguide feed," *IEEE Trans. Antennas Propagat.* vol. AP-27, pp. 279–282, Mar. 1979.
[5] S. F. Mahmoud and M. S. Aly, "A new version of dielectric lined waveguide with low cross polarization," *IEEE Trans. Antennas Propagat.* vol. AP-35, pp. 210–212, Feb. 1987.
[6] P. McCormack, "Propagation characteristics of a corrugated dielectric lined circular waveguide feed," M. S. thesis, University of Lowell, Lowell, MA, Apr. 1988.

Asymmetrical Coplanar Waveguide with Finite Metallization Thickness Containing Anisotropic Media

Toshihide Kitazawa and Tatsuo Itoh

Abstract—**The spectral-domain approach (SDA) is extended in the present paper for symmetrical and asymmetrical coplanar waveguides with anisotropic media. The quasi-static and the hybrid-mode analytical method are developed in the spectral domain taking the metallization thickness effect into consideration. Numerical computations include the quasi-static and frequency-dependent hybrid-mode values of the phase constants and characteristic impedances for the symmetrical and asym-**

Manuscript received August 14, 1990; revised March 18, 1991. This work was supported by the Texas Advanced Technology Program and by the Army Research Office under Contract DAAL03-88-K-0005.

T. Kitazawa was with the Department of Electrical and Computer Engineering, University of Texas at Austin, Austin, TX, on leave from the Department of Electronic Engineering, Kitamai Institute of Technology, Kitami, 090 Japan. He is now with the Kitami Institute of Technology.

T. Itoh was with the Department of Electrical and Computer Engineering, University of Texas at Austin, Austin, TX. He is now with the Department of Electrical Engineering, University of California at Los Angeles, Los Angeles, CA 90024.

IEEE Log Number 9101013.

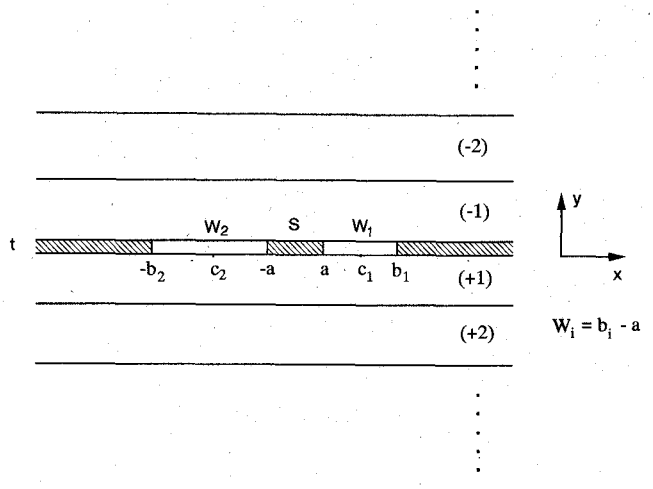

Fig. 1. Asymmetrical coplanar waveguide.

metrical CPW's and the metallization thickness effects in CPW's. Increased metallization thickness significantly reduces the nonreciprocal properties in CPW with magnetized ferrite and additional dielectric layers.

I. Introduction

Coplanar waveguides (CPW's) with anisotropic substrates have been investigated for use in microwave and millimeter-wave integrated circuits [1]–[4]. A number of theoretical analyses of CPW have been reported based on the quasi-static approach [2], [3] and the frequency-dependent hybrid-mode approach [2], [4]. However, most of these efforts have been based on the assumption that the metallization thickness is zero, and have treated the symmetrical CPW. The metallization thickness effect of CPW's in general, is larger than that of striplines because of the field configurations [3], [5], [6]. The effects have been investigated by one of the authors for the symmetrical CPW with isotropic [2] and/or uniaxially anisotropic media [3]. The asymmetrical version of the coplanar waveguide (ACPW) has been introduced to take advantage of the additional flexibility offered by the asymmetric configuration in the design of integrated circuits [7], [8]. However, there is no analytical method applicable to ACPW with finite metallization thickness.

In this paper we extend the spectral-domain approach (SDA) [9], [10] to analyze the asymmetrical coplanar waveguide (ACPW) with anisotropic media, taking the finite metallization thickness into consideration. Anisotropic media may be dielectric, e.g., sapphire and/or magnetic, e.g., magnetized ferrite. In what follows, the quasi-static as well as the hybrid-mode analytical method is developed in the spectral domain. The frequency dependence of the line parameters of CPW's is smaller than that of slotlines and striplines, and the quasi-static approximation gives reasonable results in the lower frequency range. Numerical computations are carried out for symmetrical and asymmetrical CPW's with uniaxially anisotropic dielectrics and magnetized ferrites, demonstrating the effect of the metallization on the phase constant and characteristic impedance.

II. Analytical Formalism of Electromagnetic Fields

Fig. 1 shows the cross section of an ACPW. The structure consists of printed conductors of finite thickness t with layered lossless anisotropic media. Anisotropic media of practical importance are uniaxially or biaxially anisotropic dielectrics, e.g. sapphire, and magnetized ferrites. When the layer is made of an anisotropic dielectric of this type, the permittivity tensor is expressed as

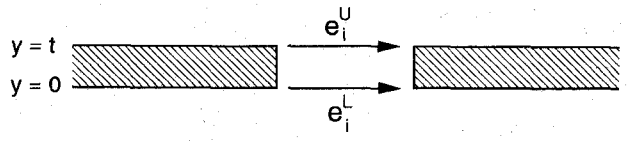

Fig. 2. Aperture fields.

$$\bar{\bar{\epsilon}} = \epsilon_0 \begin{bmatrix} \epsilon_1 & 0 & 0 \\ 0 & \epsilon_2 & 0 \\ 0 & 0 & \epsilon_3 \end{bmatrix}. \tag{1}$$

When the layer is the ferrite and is magnetized in the x direction, the permeability tensor is expressed as [9]

$$\bar{\bar{\mu}} = \mu_0 \begin{bmatrix} 1 & 0 & 0 \\ 0 & \mu_r & j\kappa \\ 0 & -j\kappa & \mu_r \end{bmatrix} \tag{2}$$

where μ_r and κ are dependent on the operating frequency ω, the applied dc magnetic field H_0, and magnetization of the ferrite $4\pi M_s$:

$$\mu_r = 1 - \frac{\gamma^2 H_0 4\pi M_s}{\omega^2 - (\gamma H_0)^2} \qquad \kappa = \frac{\gamma 4\pi M_s \omega}{\omega^2 - (\gamma H_0)^2}. \tag{3}$$

Electromagnetic fields in the aperture region ($t > y > 0$) are expressed by the Fourier series representation with respect to the x direction, viz.,

$$E_{ix}^{(0)}(x,y,z) = \frac{1}{\sqrt{2W_i}} \sum_{n=-\infty}^{\infty} \tilde{E}_{ix}^{(0)}(y) e^{-j\alpha_{in}(x-c_i)} e^{-j\beta z}, \qquad i = 1,2 \tag{4}$$

where β is the phase constant, c_i represents the center of the right ($i=1$) or left ($i=2$) aperture, and the Fourier variables α_{in} in the aperture region are determined so that the boundary conditions at the conductors are satisfied:

$$\alpha_{in} = \frac{n\pi}{W_i}. \tag{5}$$

Fields in the other open regions are expressed by the Fourier integral representation in the x direction, e.g.,

$$E_x^{(m)}(x,y,z) = \frac{1}{\sqrt{2\pi}} \int_{-\infty}^{\infty} \tilde{E}_x^{(m)}(y) e^{-j\alpha x} d\alpha\, e^{-j\beta z}$$

$$(m = \pm 1, \pm 2, \pm 3, \cdots). \tag{6}$$

Applying the continuity conditions at the interfaces and introducing the aperture fields at $y = t$, $e_i^U(x)$ and at $y = 0$, $e_i^L(x)$ (Fig. 2), the electromagnetic fields in the subregions can be

related to the aperture fields $e_t^U(x)$ and $e_t^L(x)$:

$$E^{(m)}(x,y,z)=\sum_t\int_{x_t'}\left\{\bar{\bar{T}}_{Ut}^{(m)}(x,y|x')e_t^U(x')+\bar{\bar{T}}_{Lt}^{(m)}(x,y|x')e_t^L(x')\right\}dx'e^{-j\beta z} \quad (7)$$

$$H^{(m)}(x,y,z)=\sum_t\int_{x_t'}\left\{\bar{\bar{Y}}_{Ut}^{(m)}(x,y|x')e_t^U(x')+\bar{\bar{Y}}_{Lt}^{(m)}(x,y|x')e_t^L(x')\right\}dx'e^{-j\beta z} \quad (8)$$

where the $\bar{\bar{T}}$'s and $\bar{\bar{Y}}$'s are the dyadic Green's functions.

A similar procedure is applicable for the quasi-static case. In the quasi-static approximation ($\omega\to 0$), the electric fields in each region can be expressed in terms of the x components of the aperture fields:

$$E^{(m)}(x,y)=\sum_t\int_{x_t'}\left\{R_{Ut}^{(m)}(x,y|x')e_{tx}^U(x')+R_{Lt}^{(m)}(x,y|x')e_{tx}^L(x')\right\}dx' \quad (9)$$

and the magnetic fields in each region can be expressed in terms of the y components of the magnetic flux densities at $y=t, b_{ty}^U(x)$ and at $y=0, b_{ty}^L(x)$:

$$H^{(m)}(x,y)=\sum_t\int_{x_t'}\left\{S_{Ut}^{(m)}(x,y|x')b_{ty}^U(x')+S_{Lt}^{(m)}(x,y|x')b_{ty}^L(x')\right\}dx'. \quad (10)$$

A. Quasi-Static Formulation

Quasi-static characteristics of transmission lines can be expressed in terms of the inductances and capacitances. The stationary expressions for inductances and capacitances are derived in the following.

The total current I_0 on the center strip $-a<x<a$ can be evaluated by

$$I_0=I(x_1,x_2)=\int_{x_2}^{x_1}\left\{H_x^{(+1)}(x,y=-0)-H_x^{(-1)}(x,y=t+0)\right\}dx+\int_0^t\left\{H_{1y}^{(0)}(x=x_1,y)-H_{2y}^{(0)}(x=x_2,y)\right\}dy \quad (11)$$

where x_1 lies within the right aperture $a<x_1<b_1$ and x_2 lies within the left aperture $-b_2<x_2<-a$. Multiplying (11) by $b_{1y}^U(x_1)$ and integrating over the right aperture $a<x_1<b_1$, we obtain

$$-I_0\Phi_0=\int_a^{b_1}b_{1y}^U(x_1)I(x_1,x_2)\,dx_1 \qquad (-b_2<x_2<-a) \quad (12)$$

where Φ_0 is the total magnetic flux through the aperture, i.e.,

$$\Phi_0=\int_a^{b_1}b_{1y}^U(x)\,dx=-\int_{-b_2}^{-a}b_{2y}^U(x)\,dx=\int_a^{b_1}b_{1y}^L(x)\,dx=-\int_{-b_2}^{-a}b_{2y}^L(x)\,dx. \quad (13)$$

Then, multiplying (12) by $b_{2y}^U(x_2)$ and integrating over the left aperture $-b_2<x_2<-a$, we get

$$-I_0\Phi_0^2=\int_{-b_2}^{-a}\int_a^{b_1}b_{1y}^U(x_1)I(x_1,x_2)b_{2y}^U(x_2)\,dx_1\,dx_2. \quad (14)$$

Substituting (10) and (11) into (14) and using (13), we get

$$\frac{1}{L}=\frac{I_0}{\Phi_0}=\left(\frac{1}{L}\right)_U+\left(\frac{1}{L}\right)_L+\left(\frac{1}{L}\right)_{\Delta R}+\left(\frac{1}{L}\right)_{\Delta L} \quad (15)$$

where the subscripts U, L, ΔR, and ΔL stand for the contributions from the upper ($y>t$) and lower ($y<0$) half regions and the right and left aperture regions, respectively; they are expressed as

$$\left(\frac{1}{L}\right)_U=\sum_t\int\int_{x_t}b_{ty}^U(x)G_U(x|x')\cdot b_{ty}^U(x')\,dx'\,dx\left\{\int_a^{b_1}b_{ty}^U(x)\,dx\right\}^{-2} \quad (16)$$

and

$$\left(\frac{1}{L}\right)_{\Delta R}=\int\int_a^{b_1}\left\{b_{1y}^U(x)G_s(x|x')b_{1y}^U(x')+b_{1y}^L(x)G_s(x|x')b_{1y}^L(x')+b_{1y}^U(x)G_m(x|x')b_{1y}^L(x')\right\}dx'\,dx\left\{\int_a^{b_1}b_{ty}^U(x)\,dx\right\}^{-2}. \quad (17)$$

The expressions for $(1/L)_L$ and $(1/L)_{\Delta L}$ are similar to (16) and (17), respectively. Equations (16) and (17) are stationary and they give the lower bounds on the inductances.

The stationary expressions for the capacitances are derived in similar fashion. Instead of the total current I_0, the total charge Q_0 on the center strip $-a<x<a$ plays an important role in this case:

$$Q_0=Q(x_1,x_2)=\int_{x_2}^{x_1}\left\{D_y^{(-1)}(x,y=t+0)-D_y^{(+1)}(x,y=-0)\right\}dx+\int_0^t\left\{D_{1x}^{(0)}(x=x_1,y)-D_{2x}^{(0)}(x=x_2,y)\right\}dy. \quad (18)$$

Multiplying (18) by $e_{1x}^U(x_1)$ and $e_{2x}^U(x_2)$ and integrating over the right aperture $a<x_1<b_1$ and the left aperture $-b_2<x_1<-a$, we obtain

$$-Q_0V_0^2=\int_{-b_2}^{-a}\int_a^{b_1}e_{1x}^U(x_1)Q(x_1,x_2)e_{2x}^U(x_2)\,dx_1\,dx_2 \quad (19)$$

where V_0 is the potential difference between the center strip and the ground conductors, i.e.,

$$V_0=-\int_a^{b_1}e_{1x}^U(x)\,dx=\int_{-b_2}^{-a}e_{2x}^U(x)\,dx=-\int_a^{b_1}e_{1x}^L(x)\,dx=\int_{-b_2}^{-a}e_{2x}^L(x)\,dx. \quad (20)$$

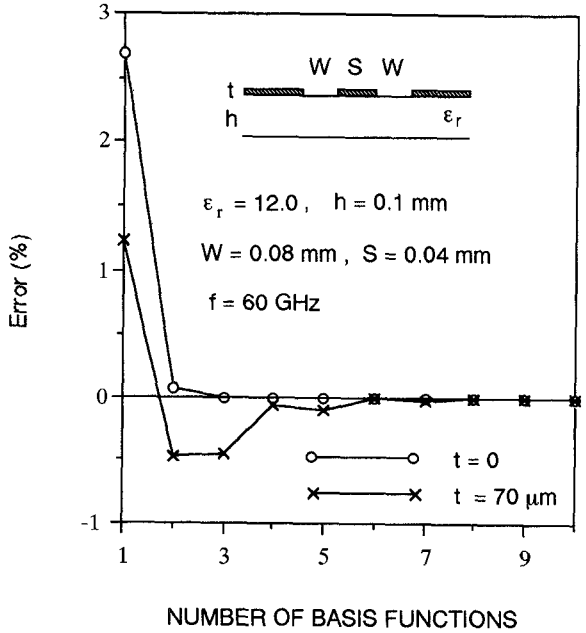

Fig. 3. Convergence of calculated results.

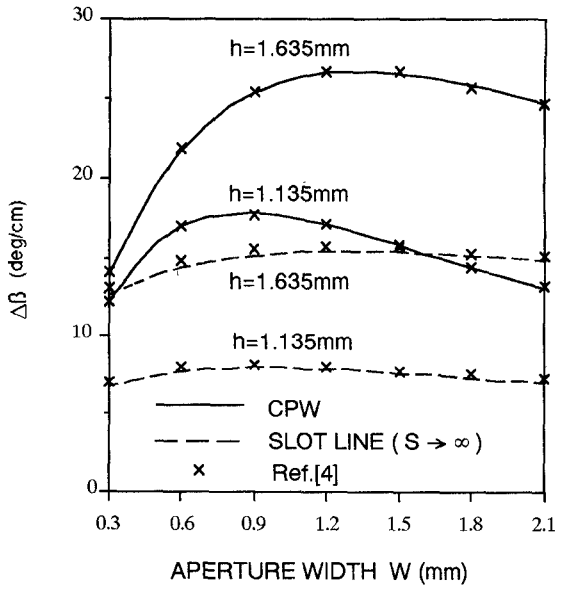

Fig. 4. Differential phase shift of single-layered slotline and coplanar waveguide: $\epsilon_F = 11.6$, $f = 10$ GHz, $M_s = 1800$ A/cm, $H_0 = 300$ A/cm, $S = \frac{4}{3}W$ (CPW), $S \to \infty$ (slotline).

Substituting (9) and (18) into (19) and using (20), we get

$$C = \frac{Q_0}{V_0} = C_U + C_L + C_{\Delta R} + C_{\Delta L} \tag{21}$$

where the expressions for C_U, C_L, $C_{\Delta R}$, and $C_{\Delta L}$ are similar to those for the $(1/L)$'s and they have stationary properties. It should be noted that the sum of C_U and C_L corresponds to the total capacitance of CPW with zero metallization thickness, and that the metallization thickness effect is accounted for mainly by $C_{\Delta R}$ and $C_{\Delta L}$.

B. Hybrid-Mode Formulation

Applying the continuity conditions of the magnetic fields at the aperture surface $y = t$ and 0 to expression (8), we obtain the integral equations for the aperture fields $e_t^U(x)$, $e_t^L(x)$ and implicitly the propagation constant β. Then, applying Galerkin's procedure [2], [4]–[7], [9], [10] to the integral equations, we obtain the determinantal equation for β. In this procedure, the unknown aperture fields $e_t^U(x)$, $e_t^L(x)$ are expanded in terms of the appropriate basis functions:

$$e_{tx}^U(x') = \sum_{k=1}^{N_x} a_{txk} f_{txk}(x) \qquad e_{tx}^L(x') = \sum_{k=1}^{N_x} b_{txk} f_{txk}(x)$$
$$e_{ty}^U(x') = \sum_{k=1}^{N_y} a_{tyk} f_{tyk}(x) \qquad e_{ty}^L(x') = \sum_{k=1}^{N_y} b_{tyk} f_{tyk}(x). \tag{22}$$

Taking the edge effect into consideration, the basis functions are defined as [2]

$$f_{txk}(x) = \frac{T_k\left\{\dfrac{2(x-c_t)}{W_t}\right\}}{\sqrt{1-\left\{\dfrac{2(x-c_t)}{W_t}\right\}^2}}$$
$$f_{tyk}(x) = U_k\left\{\frac{2(x-c_t)}{W_t}\right\} \tag{23}$$

where $T_k(x)$ and $U_k(x)$ are Chebyshev polynomials of the first and second kind, respectively.

III. Numerical Examples

Some preliminary computations are carried out for the special cases of CPW's to show the validity of the present method. Fig. 3 shows the convergence of the calculated results with respect to the number of basis functions. The effective dielectric constants, defined as

$$\epsilon_{\text{eff}} = \left(\beta / \omega\sqrt{\epsilon_0 \mu_0}\right)^2 \tag{24}$$

are calculated for the simple structures of symmetrical CPW's with isotropic substrates. The number of basis functions is increased to $N = 10$, and the percentage error to the value of the $N = 10$ case is shown in the figure. Rapid convergence is observed for both the zero and the finite thickness case. The isotropic substrate of the configuration shown in Fig. 3 is replaced by the magnetized ferrite, and the differential phase shift $\Delta\beta = \beta_f - \beta_r$ is calculated in Fig. 4 together with the published data [4] for the case with zero metallization thickness ($t = 0$). Close agreement between the two sets of results is observed for a wide range of aperture widths.

Fig. 5 shows the frequency-dependent characteristics of the symmetrical and the asymmetrical CPW with an anisotropic sapphire substrate. The figure includes the numerical results of the effective dielectric constants (Fig. 5(a) and (b)) and the characteristic impedances (Fig. 5(c)). It should be noted that the thickness effect of the c-mode case is smaller than that of the π-mode case (Fig. 5(b)). In the π-mode case, the electric field lines run between the center strip and semi-infinite conductors, while in the c-mode case, the electric field lines run between the semi-infinite conductors too; therefore the fractional flux in the aperture region ($t > y > 0$) becomes smaller in the c-mode case. The definition for the frequency-dependent characteristic im-

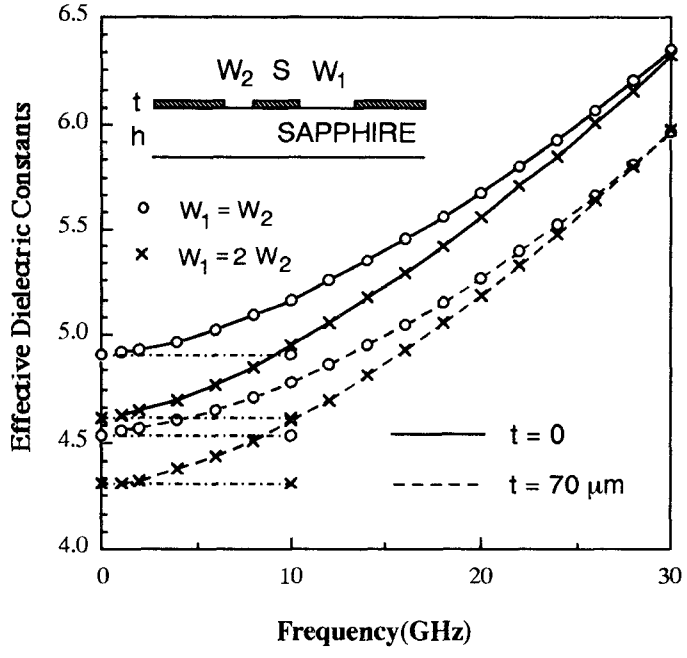

(a)

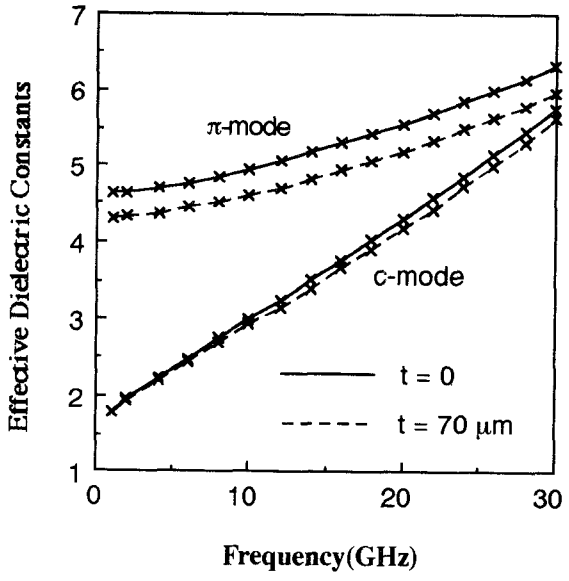

(b)

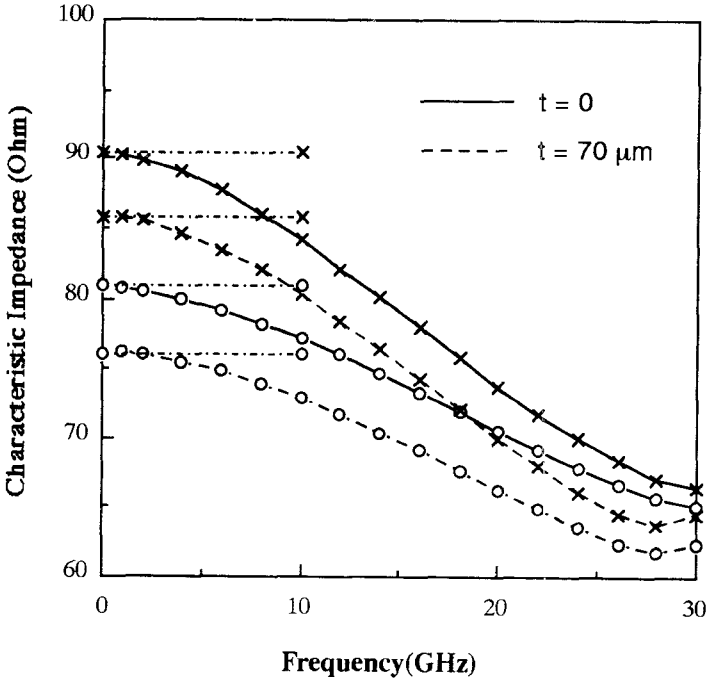

(c)

Fig. 5. Frequency-dependent characteristics of CPW with anisotropic sapphire substrate. (a) Frequency dependence of symmetrical and asymmetrical CPW. (b) Frequency dependence of the π and c modes. (c) Characteristic impedance. $h = 1$ mm, $W_2 = 1$ mm, $S = 0.5$ mm, $\epsilon_1 = \epsilon_3 = 9.4$, $\epsilon_2 = 11.6$:

—o— symmetrical CPW ($W_1 = W_2$);

—×— asymmetrical CPW ($W_1 = 2W_2$);

quasi-static values.

pedance is not uniquely specified for the hybrid-mode propagation. For the symmetrical coplanar waveguide, it has been evaluated by the power–voltage basis [2]:

$$Z_{PV} = \frac{V_0^2}{P_0} \tag{25}$$

where P_0 is the average power flow in the z direction, and V_0 is the voltage difference between the center strip and the ground conductors. However, for the asymmetrical case, the voltage difference between the center strip and the ground conductors is not uniquely specified except at zero frequency (the quasi-static case, eq. (20)); in general,

$$\int_a^{b_1} e_{1x}^U(x)\,dx \neq -\int_{-b_2}^{-a} e_{2x}^U(x)\,dx. \tag{26}$$

To avoid ambiguity, we chose the following definition:

$$Z_{PI} = \frac{P_0}{I_0^2} \tag{27}$$

where I_0 is the total current on the center strip $-a < x < a$ and it can be evaluated accurately by using a procedure similar to that used in deriving the stationary expression for the quasi-static case. Multiplying (11) by $e_1^U(x_1)$ and $e_2^U(x_2)$ and integrating over the right aperture $a < x_1 < b_1$ and the left aperture $-b_2 < x_2 < -a$, we obtain

$$I_0 = \int_{-b_2}^{-a}\int_a^{b_1} e_{1x}^U(x_1) I(x_1, x_2) e_{2x}^U(x_2) \cdot dx_1\,dx_2 \left\{\int_a^{b_1} e_{1x}^U(x)\,dx\right\}^{-1} \left\{\int_{-b_2}^{-a} e_{2x}^U(x)\,dx\right\}^{-1}. \tag{28}$$

Frequency-dependent hybrid-mode values converge to the corresponding quasi-static values in the lower frequency range for all cases.

Fig. 6 shows the dispersion characteristics of the ACPW with the magnetized ferrite with zero and finite metallization thicknesses. The nonreciprocal properties as well as the metallization thickness effect are demonstrated in the figure. The metallization thickness effect in the forward waves is larger than that in the backward waves because of the difference of the field distribution between the forward and backward waves, which increases the nonreciprocity slightly in this configuration.

Planar waveguides with a single-layered ferrite substrate do not exhibit adequate nonreciprocity, and additional layers, such as spacer or overlay (Fig. 7), are introduced to increase the nonreciprocity [4], [9], [11]. In the layered structures with overlay or spacer of high permittivity near the line conductor, the electromagnetic fields are concentrated near the line conductor edge, which may increase the effect of the conductor thickness. Parts (a) and (b) of Fig. 8 show the frequency dependence of the differential phase shift $\Delta\beta = \beta_f - \beta_r$ for CPW's with a dielectric spacer (the double-layered CPW) and a dielectric overlay (the sandwich CPW), respectively. The numerical results for the CPW's with zero ($t = 0$) and finite ($t = 70$ μm) thicknesses of the metallization are plotted together with the published data [4]. The good agreement between the values of the zero metallization thickness obtained by the present method and those in [4] is observed. The phase constants of the backward β_r and forward β_f waves are lowered by the finite metallization thickness, but the metallization thickness effect in the backward waves is larger than in the forward waves because of the difference of the field distribution, which decreases the nonreciprocity significantly in these configurations. Parts (c) and (d) of Fig. 8 show the variation of the differential phase shift with the metallization thickness for the double-layered CPW and the sandwich CPW, respectively.

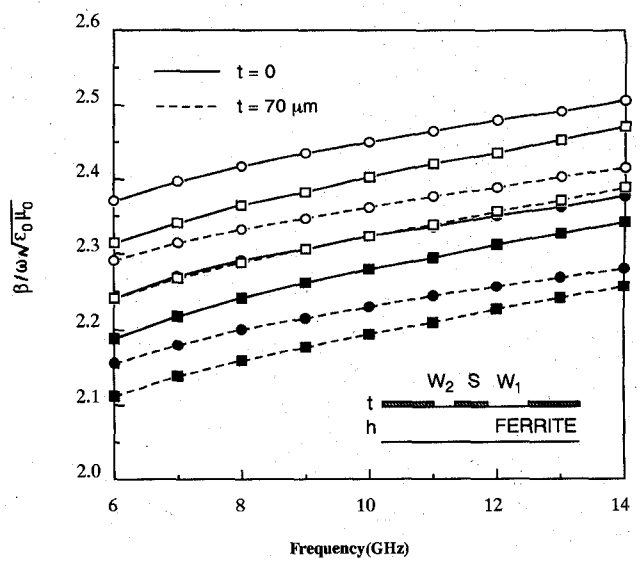

Fig. 6. Dispersion characteristics of ACPW with magnetized ferrite: $h = 1$ mm, $W_2 = 1$ mm, $S = 0.5$ mm, $\epsilon_F = 11.6$, $M_s = 1800$ A/cm, $H_0 = 300$ A/cm:

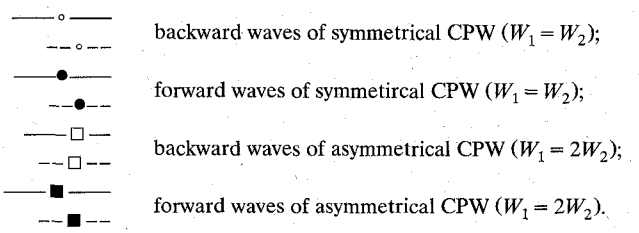

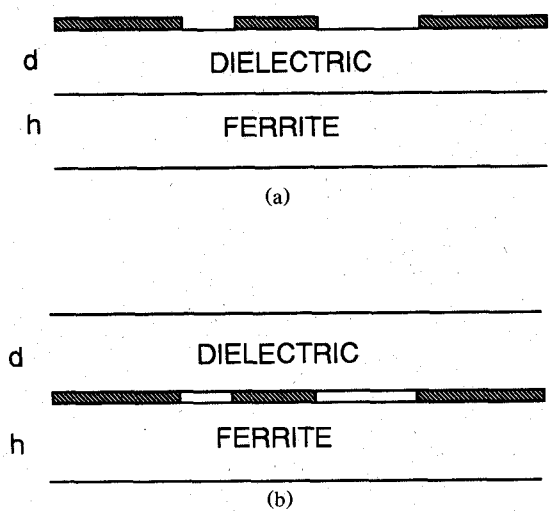

Fig. 7. (a) ACPW with ferrite and dielectric spacer (double-layered ACPW). (b) ACPW with ferrite and dielectric overlay (sandwich ACPW).

IV. Conclusions

The spectral-domain approach (SDA) is extended in the present paper for the symmetrical and the asymmetrical coplanar waveguide with anisotropic media. Quasi-static and hybrid-mode

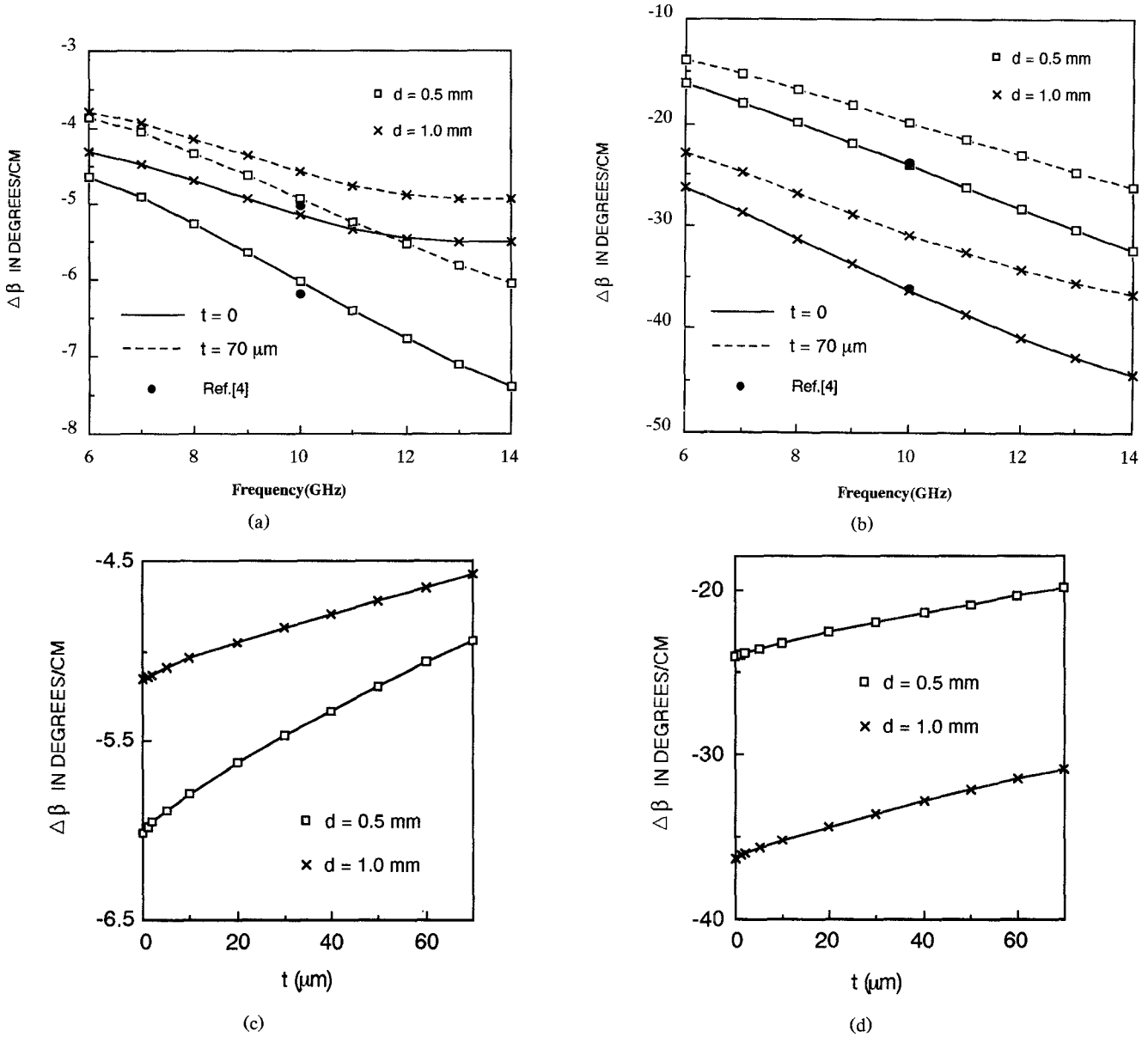

Fig. 8. (a) Differential phase shift of double-layered CPW. (b) Differential phase shift of sandwich CPW. (c) Effect of metallization thickness of double-layered CPW. (d) Effect of metallization thickness of sandwich CPW. $h = 0.635$ mm, $W_1 = W_2 = 1.27$ mm, $S = 1.7$ mm, $\epsilon_F = 11.6$, $M_s = 1800$ A/cm, $H_0 = 300$ A/cm, $\epsilon_D = 20$:

—□— / --□-- $d = 0.5$ mm;

—×— / --×-- $d = 1.0$ mm;

• ref. [4].

analytical methods are developed in the spectral domain taking the metallization thickness effect into consideration. The quasi-static formulation presents expressions for the line capacitance and inductance in variational form. The frequency-dependent hybrid-mode values of the phase constants and characteristic impedances converge to the quasi-static values for the symmetrical and asymmetrical CPW's with uniaxially anisotropic media for both zero and finite metallization thicknesses. The metallization thickness effects are demonstrated for the first time for CPW's with anisotropic dielectric and magnetic media. The effects are different for the π- and c-mode cases. Increased metallization thickness reduces significantly the nonreciprocal properties in CPW with magnetized ferrite and additional layers which are introduced to increase the nonreciprocity. Evaluation of the losses caused by ferrite and finite conductivities of the conductors is a topic for future work.

References

[1] C. P. Wen, "Coplanar waveguide: A surface strip transmission line suitable for nonreciprocal gyromagnetic device applications," *IEEE Trans. Microwave Theory Tech.*, vol. MTT-17, pp. 1087–1090, Dec. 1969.

[2] T. Kitazawa and Y. Hayashi, "Coupled slots on an anisotropic sapphire substrate," *IEEE Trans. Microwave Theory Tech.*, vol. MTT-29, pp. 1035–1040, Oct. 1981.
[3] T. Kitazawa and Y. Hayashi, "Quasistatic characteristics of a coplanar waveguide with thick metal coating," *Proc. Inst. Elect. Eng., (Microwaves Antennas Propagat.)*, vol. 133, no. 1, pp. 18–20, Feb. 1986.
[4] E. El-Sharawy and R. W. Jackson, "Coplanar waveguide and slot line on magnetic substrates: Analysis and experiment," *IEEE Trans. Microwave Theory Tech.*, vol. 36, pp. 1071–1978, June 1988.
[5] T. Kitazawa, "Metallization thickness effect of striplines with anisotropic media: Quasi-static and hybrid-mode analysis," *IEEE Trans. Microwave Theory Tech.*, vol. 37, pp. 769–775, Apr. 1989.
[6] T. Kitazawa, Y. Hayashi, and M. Suzuki, "A coplanar waveguide with thick metal coating," *IEEE Trans. Microwave Theory Tech.*, vol. MTT-24, pp. 604–608, Sept. 1976.
[7] T. Kitazawa and Y. Hayashi, "Analysis of asymmetrical coplanar waveguide and coplanar strip lines with anisotropic substrate," *Electron. Lett.*, vol. 21, pp. 986–987, 1985.
[8] T. Kitazawa and R. Mittra, "Quasistatic characteristics of asymmetrical and coupled coplanar-type transmission lines," *IEEE Trans. Microwave Theory Tech.*, vol. MTT-33, pp. 771–778, 1985.
[9] M. Geshiro, and T. Itoh, "Analysis of double-layered finlines containing a magnetized ferrite," *IEEE Trans. Microwave Theory Tech.*, vol. MTT-35, pp. 1377–1381, Dec. 1987.
[10] T. Itoh and R. Mittra, "Spectral-domain approach for calculating the dispersion characteristics of microstrip line," *IEEE Trans. Microwave Theory Tech.*, vol. MTT-21, pp. 496–499, 1973.
[11] G. Bock, "New multilayered slot-line structures with high nonreciprocity," *Electron. Lett.*, vol. 19, no. 23, pp. 966–968, Nov. 1983.

Quasi-Static Analysis of Three-Line Microstrip Symmetrical Coupler on Anisotropic Substrates

Lukang Yu and Banmali Rawat

Abstract—**A method for analyzing the three symmetrically coupled microstrip lines on an anisotropic substrate has been developed. Computer programs based on the method of moments have been employed and the coupler mode impedance, Z, coupling constant, K, and phase velocity, v, as functions of the anisotropy ratio, $\epsilon_{xx}/\epsilon_{yy}$, have been obtained.**

I. Introduction

Three-line microstrip couplers are an integral part of many microwave communication systems, such as six-port reflectometers, balanced mixers, and phase shifters. In the analysis of three equal-width microstrip lines on isotropic substrates, it has been reported that under the assumption of a certain set of voltage modes, the characteristic impedance of the center line will always be the same as that of the side lines [1]. This imposes no condition on the capacitance coefficients of the network. Further work has revealed that for the same coupled system, the normal-mode impedances of the center line may be greater than those of side lines at small widths and separations; hence there are five normal-mode impedances [2]. It is necessary to increase the width of the center line relative to that of the outer lines in order to equalize the mode impedances. On the other hand, however, in the limit (W/h and $S/h > 0.8$), the two systems will be practically indistinguishable from each other.

Manuscript received October 29, 1990; revised March 19, 1991. Part of this paper was presented at the 1990 IEEE AP-S International Symposium, Dallas, TX, May 1990.

The authors are with the Department of Electrical Engineering, University of Nevada, Reno, NV 89557-0030.

IEEE Log Number 9101016.

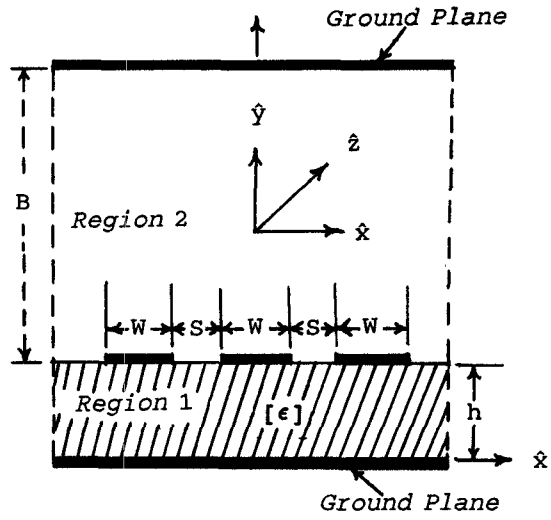

Fig. 1. Cross section of three coupled microstrip lines on an anisotropic substrate.

The boundary value problems involving single and coupled microstrip lines on anisotropic substrates such as sapphire and pyrolytic boron nitride (PBN) have been approached from numerical points of view [3]–[7]. Green's functions in the spectral domain have been utilized to transform an anisotropic problem to an isotropic one. It has been found for coupled lines that under the quasi-static TEM assumption, the difference between even- and odd-mode phase velocities can be significantly reduced by using anisotropic substrate. This implies that if an anisotropic material with a large anisotropy ratio is available, the isolation and directivity of microstrip couplers can be significantly improved.

In this paper, a system of three symmetrically coupled microstrip lines on an anisotropic substrate is analyzed. For a three-mode impedance system, the directivity of the three-line coupler is found to be improved by equalizing v_{eo} (square-root average of phase velocities of *ee* and *oo* modes) and v_{oe} (phase velocity of *oe* mode). The validity of our method has been verified by substituting the conditions of isotropic material in the equations derived for anisotropic material and then comparing the characteristic impedances with the results obtained in [1] and [2] for isotropic materials.

II. Derivation of Green's Function

The configuration of the three symmetrically coupled microstrip lines under consideration is shown in Fig. 1. It comprises three zero-thickness strips of width W and interstrip spacing S on an anisotropic dielectric substrate with thickness h. The introduction of ground cover by no means affects the solution as B is allowed to recede to infinity. In this derivation, an anisotropic substrate layer of homogeneous dielectric has been considered which has a relative permittivity tensor given by

$$\bar{\epsilon} = \epsilon_0 \begin{bmatrix} \epsilon_{11} & \epsilon_{12} \\ \epsilon_{21} & \epsilon_{22} \end{bmatrix} \tag{1}$$

0018-9480/91/0800-1433$01.00 ©1991 IEEE